

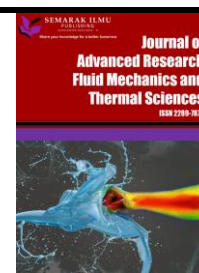


Journal of Advanced Research in Fluid Mechanics and Thermal Sciences

Journal homepage:

https://semarakilmu.com.my/journals/index.php/fluid_mechanics_thermal_sciences/index

ISSN: 2289-7879



Experimental Investigation of Nanofluid Turbulent Flow Over Microscale Backward-Facing Step

Abd. Rahim Abu Talib^{1,2,*}, Sadeq Salman³, Muhammad Fitri Mohd Zulkeple¹, Ali Kareem Hilo⁴

¹ Aerodynamic, Heat Transfer & Propulsion Group, Department of Aerospace Engineering, Universiti Putra Malaysia, 43400 Serdang, Selangor Malaysia

² Aerospace Malaysia Research Centre, Faculty of Engineering, Universiti Putra Malaysia, 43400 Serdang, Selangor, Malaysia

³ Scientific Research Center, Al-Ayen University, Nasiriyah, Iraq

⁴ Department of Naval Architecture and Ocean Engineering, Chungnam National University, Daejeon 34134, South Korea

ARTICLE INFO

Article history:

Received 15 April 2022

Received in revised form 13 August 2022

Accepted 24 August 2022

Available online 16 September 2022

Keywords:

Microscale; backward-facing step;
heat transfer; turbulent flow;
nanofluid

ABSTRACT

Experimental research was presented in this paper to illustrate the heat transmission and flow characteristics of nanofluid on a microscale backward-facing step channel. Except for the downstream wall, which was applied with uniform heat flow, the channel side walls were deemed adiabatic. Water was used as the base fluid and mixed with 30 nm diameter CuO nanoparticles with a volume fraction in the range of 0-0.04. The experiment was conducted at a Reynolds number range of 5,000–10,000. The results showed that the Nusselt number increases as the volume fraction increases. However, the increase in the nanoparticle volume fraction leads to an increment in the friction factor. Furthermore, the results indicated that increasing the Reynolds number lead to the volume fraction decreasing. It was found that there is an improvement of heat transfer by applying the CuO/water nanofluid with a 0.03 volume fraction of CuO nanoparticles with a significant performance evaluation criterion ($PEC > 1$).

1. Introduction

In some engineering applications that require heating or cooling, the flow separation and reattachment play a crucial part in the design process. The backward-facing step (BFS) has been designed in numerous applications in which heat transfer is the core, such as electronic equipment, environmental inspection systems, combustion chambers, electrical systems, flow valves, and turbine blade cooling passes. However, the flow separation phenomenon is undesirable for many engineering domains because of the loss in the energy and the pressure drop that occurs require an extra pumping power to solve them [1-7].

Many backward-facing step (BFS) studies have been conducted using different parameters and flow regimes, both experimentally and numerically. Some of these studies investigated the effects of step height (S) on the heat transfer characteristics in various flow regimes. The results of S in a BFS

* Corresponding author.

E-mail address: abdrahim@upm.edu.my

<https://doi.org/10.37934/arfmts.99.2.119134>

channel were presented by Abu-Mulaweh *et al.*, [8-11], and the study of Nie and Armaly [12], which was based on the experimental research of Armaly *et al.*, [13]. Furthermore, Chen *et al.*, [14] have examined the S in BFS in turbulent and laminar regimes. In the microscale backward-facing step (MBFS) channel, a numerical study was conducted by Kherbeet *et al.*, [15] that examined the influence of S in the regime of the laminar flow. All the mentioned studies above have revealed that the step height (S) has a significant impact on the characteristics of fluid flow and heat transfer.

In the case of nanofluid studies, many researchers have investigated the use of nanoparticles in the traditional fluids over the backward-facing step (BFS) [16-28]. The effect of the volume fractions (φ) on the heat transfer and fluid flow have been investigated. It has been proven that an increment in the Nusselt number (Nu) increases the heat transfer rate when the volume fraction (φ) is increased. Moreover, other studies have revealed that by increasing the nanoparticle φ caused a high friction factor [17,18,21,23,25,27]. On the other hand, the effect of the nanoparticle diameter was also probed. The outcomes demonstrated that the diameter of the nanoparticles has an empirical impact on heat transfer enhancement [23,28].

A large-sized eddy model was used to investigate the turbulent heat transfer in the separated flow over the backward-facing step (BFS) channel by numerous researchers [29,30]. The outcomes revealed a remarkable enhancement in the rate of the heat transfer in the recirculation area and the heat transfer coefficients. Furthermore, some studies used the Laser Doppler Velocimetry model (LDV) to examine the turbulent flow over BFS. In the study of Abu-Mulaweh *et al.*, [31], the LDV model was applied to explore the circulation of turbulent mixed convection on 2D BFS. The outcomes of their study have a notable agreement with the study of Nie and Armaly [32], which was carried out over 3D BFS.

It is worth to mention that only a few studies have been held over the laminar flow regime on the microscale backward-facing step (MBFS) channel, either experimentally or numerically [15,22,23,28,33,34]. A numerical study of the turbulent flow over MBFS has been conducted by Salman *et al.*, [35] on the effect of using different base fluids. To the best of the authors' knowledge, numerical nor experimental study has been published using turbulent nanofluid flow over MBFS [36]. The current study has nominated CuO nanoparticles and the water as base fluid to address the impact that can be caused on the rate of heat transfer. Moreover, the study showed the preparation of the nanofluid experimentally. The main objectives of the current research are to investigate experimentally the turbulent CuO/water nanofluid flow and volume fraction (φ) over MBFS. Additionally, the paper discusses the characteristics of CuO nanoparticles.

2. Methodology

2.1 Test Section and Equipment

To make sure that the channel is fully developed, the upstream and the downstream walls' lengths are set to be 80 and 100 mm, respectively. The width of the channel is 30 mm, and the height is 1000 μm . At the downstream wall, a continuous heat flux of 80 W/m^2 has been applied, while the rest of the walls are considered adiabatic. A step height (S) of 500 μm has been considered in this study. In Figure 1, the MBFS schematic diagram of the present research is demonstrated.

Figure 2 shows the experimental setup of the study. The fluid was contained in the chiller tank pushed by a water pump (Preco QB-60 1"x0.5hp Peripheral Water Pump ID30546). The tested MBFS duct was connected by fabricating two sumps at the two ends. For controlling the rate of the inlet flow on the test section and for reducing the system's high pressure, distribution valves were placed between the inlet pumps and the high-pressure pump. A micro screen filter was positioned to avoid big particles entering the test section. In order to determine the channel friction factor, a pressure

drop in the test section was calculated. Two press tapes are machined in the upstream and downstream of the test section. A pressure gauge of $\pm 0.5\%$ accuracy is attached to two taps tools. 10 mm thick acrylic materials were used in all the walls of the test section (excluding downstream wall) to ensure proper environmental insulation.

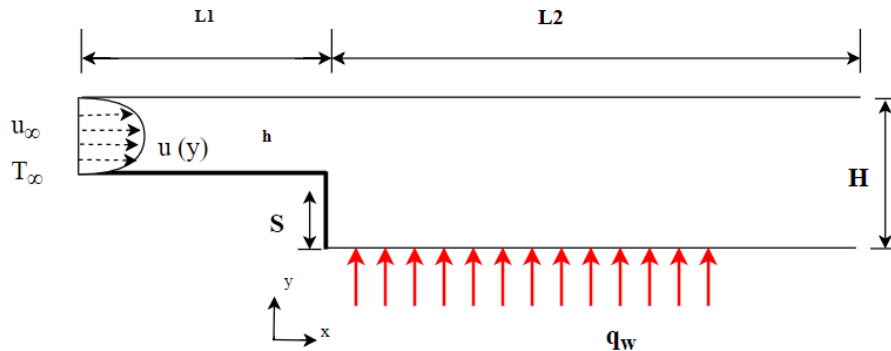
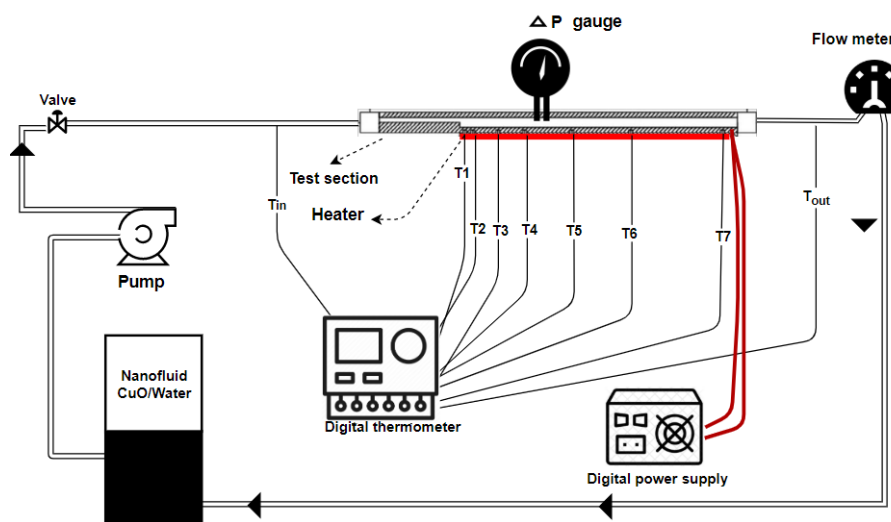
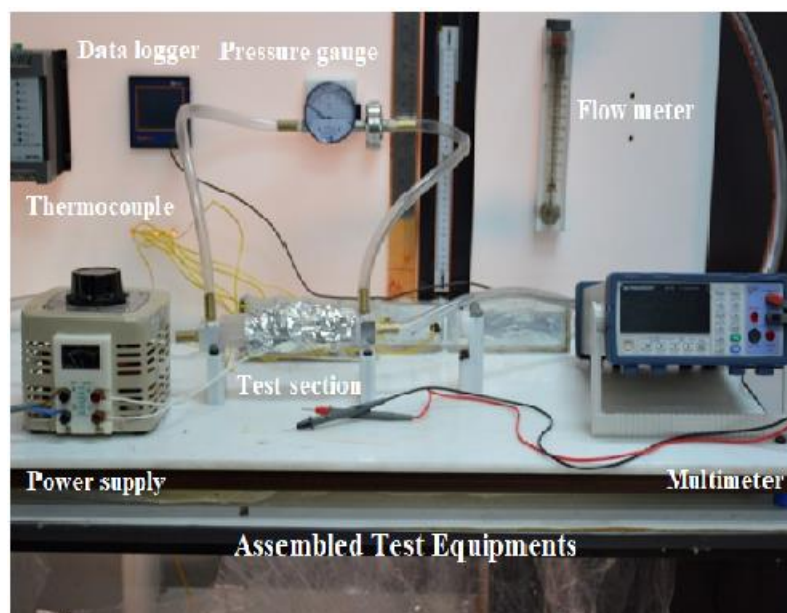


Fig. 1. Horizontal 2D microscale backward-facing step (MBFS) schematic diagram

Along the downstream wall, seven 1 mm holes were made nearest to the internal surface for inserting the thermocouples. Uniform heat flux was provided for the current experiment study at the test section downstream wall (aluminium platform) where the cartridge heater is installed. Seven holes were made and distributed over the length of the heater cartridge with a diameter of 1 mm. Also, the position of the holes is precisely the same as the location of the holes at the downstream wall. The holes are constructed to connect the wires of the thermocouple to the downstream wall over the cartridge heater and near to the internal surface. This heater has a working temperature range of 0–150°C.



(a)



(b)

Fig. 2. Experimental setup (A) schematic diagram (B) assembled test equipment

The electricity supply regulator, which has the input voltage controller, is connected to the heater. On the downstream wall, there are seven 1 mm-diameter of type-K thermocouples with an accuracy of $\pm 1\%$ installed. Both the outlet and the inlet of the test duct are also attached to two thermocouples to indicate the temperature for the whole experimental operation, and the seven thermocouples are connected to the downstream from the outside along the flow direction to show the wall temperature in the heat transfer progression.

In order to reduce the losses of the heat flux to the environment, isolation is employed to contain the outside of the heater cartridge. The flow meter, which is used to measure the mass flow rate of the fluid flow, is placed at the test section outlet. The Reynolds number (Re) is varied from 5,000 to 10,000 during the experiment. After the flow meter, the fluid coming out of the test channel was returned to the chiller tank.

2.2 CuO Nanoparticle Characterisation

Scanning electron microscopy (SEM) was used to characterise the CuO nanoparticles and their morphology before the experiment. Furthermore, the CuO nanoparticles' crystalline phases were obtained by x-ray diffraction patterns (XRD). In the first step, dry CuO nanoparticles were used in the preparation of the nanofluid to obtain the characterisation. The SEM was achieved using a Hitachi S-3400 N equipment. For electricity conduction, a thin golden layer was applied as a coat to the sample before the scanning. Then, a 20 kV voltage was applied to generate electron bundles in a high vacuum. The sample topography and the high-resolution images were obtained by sending signals from the generated electrons. A regular SEM of CuO nanoparticles' micrograph is demonstrated in Figure 3.

The CuO particle size and the morphology are visible. It evident that the CuO particles are nearly spherical. The particle size distributions of the CuO nanoparticles are like those obtained by the SEM. The CuO particle size distribution is shown in Figure 4.

A 2500 x-ray diffractometer has been used for the CuO nanoparticle analysis of the XRD diffraction. The range of the angular scattering (2θ) was from 20° to 70° , and 0.02 degrees per angle

was the speed rate. 35 mA and 40 kV were the operating current and voltage during the test. The typical CuO nanoparticle XRD patterns are shown in Figure 5.

The impurity peaks have been observed only for CuO particles. The Debye–Scherrer’s formula to calculate the average crystallite size of the CuO nanoparticles is as follows [37]:

$$D = \frac{k\lambda}{\beta \cos \theta} \quad (1)$$

Where the particle size (nm) is D , the x-ray radiation wavelength is λ (which is equal to 1.5406 nm), the full width at half maximum of the peak is β (in radians), k is a constant (which is equal to 0.94), and the Bragg angle is 2θ . Applying Eq. (1), the size of the particle can be calculated in every single peak of the diffraction. The XRD analysis outcomes are consistent with the literature of the monoclinic CuO (JCPDS 45-0397). The CuO particles size distribution is 30.7 nm for the (111) peaks.

In the current research, the nanofluid heat transfer and flow characteristics were examined over the MBFS. As employing nanofluids in MBFS can increase the pressure drop in addition to enhancing the heat transfer, the optimal situation of a minimum pressure drops, and maximum heat transfer can be obtained by applying optimisation methods. The nanoparticle size and the volume fraction (φ) have significant effects on the nanofluid's characteristics on MBFS, which demand a high pumping power. These challenges should be assessed in future studies.

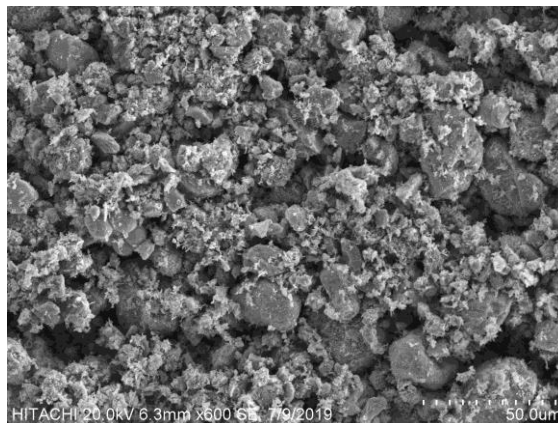


Fig. 3. SEM images of CuO nanoparticles show spherical shapes

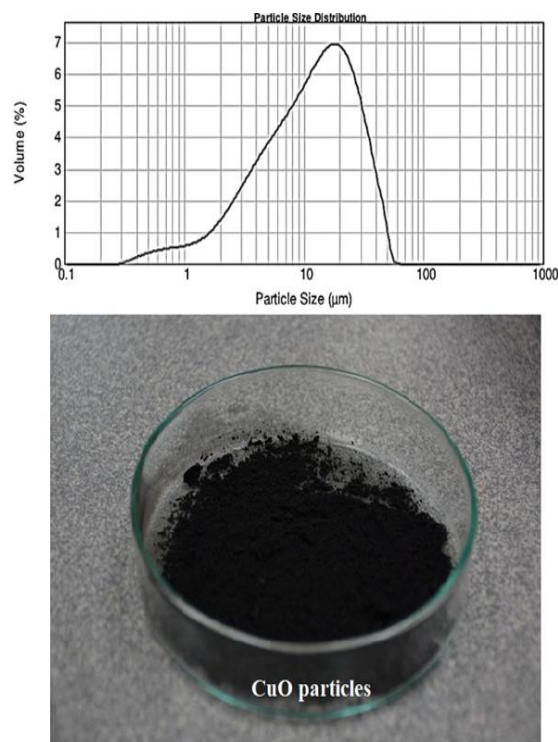


Fig. 4. CuO nanoparticles' particle size distribution

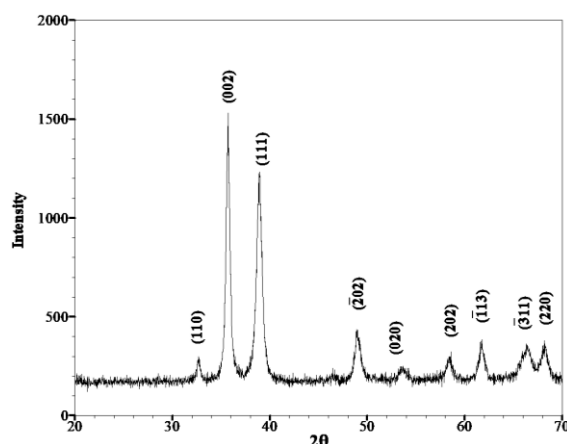


Fig. 5. XRD of CuO nanoparticles

2.3 Nanofluid Preparation

The CuO nanopowder was manufactured by Wuhan Dongxin Mill Imp & Exp Trade Co. Ltd. using the method of physical vapour synthesis. The two-step method has been applied in the dispersion of the nanoparticles in the base fluids. The adopted nanoparticle material is CuO, with a diameter of 40 nm and spherical shape.

A balance with a high sensitivity of 0.1 mg resolution (HR-250 AZ compact analytical balance) is used to carefully weigh the nanoparticles. From Eq. (2), the volume fraction (φ) of the current study is obtained [26]. By adding the determined quantity of the nanoparticles in a known quantity of water, the nanofluid is prepared. To improve the nanoparticle dispersion in the water, a 700 W 40 kHz POWER SONIC 420 is used to sonicate the nanofluid for six hours.

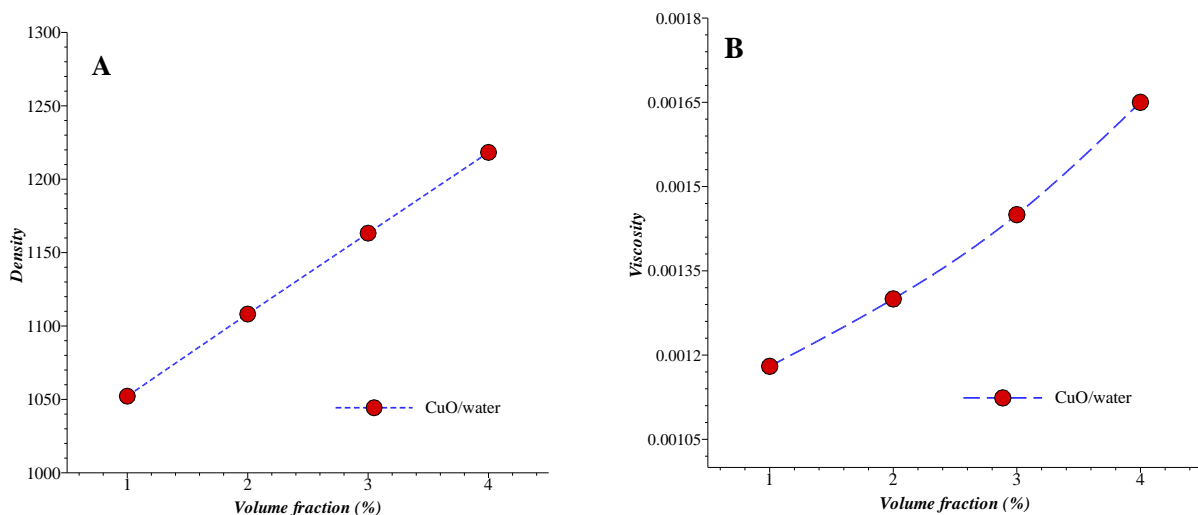
$$\varphi = \frac{\left[\frac{w_{particle}}{\rho_{particle}} \right]}{\left[\frac{w_{particle}}{\rho_{particle}} + \frac{w_{basefluid}}{\rho_{basefluid}} \right]} \quad (2)$$

It can be confirmed that there is no sedimentation, and the agglomerated nanoparticles are dispersed into the base fluid evenly. The colour of the prepared liquid is dark brown. The nanofluid and various volume fractions (φ) are portrayed in Figure 6.



Fig. 6. Samples of CuO/water nanofluids at different volume fractions (φ)

CuO/water thermophysical properties have been obtained experimentally at different volume fraction as it is showing in Figure 7. Figure 7(A) presents the density outputs which has been obtained by balancing the specific nanofluid volume. Also, the viscosity has been obtained by utilizing the viscometer as it demonstrated in Figure 7(B). Moreover, by employing different scanning calorimeter (DSC), the specific heat (CP) has been calculated as it is showing in Figure 7(C). To calculate the thermal conductivity KD2 has been used to measure the thermal conductivity of different volume fraction. Figure 7(D) demonstrated the results of the thermal conductivity. It is worth to mention that the water has been used to check the accuracy of the devices that been used.



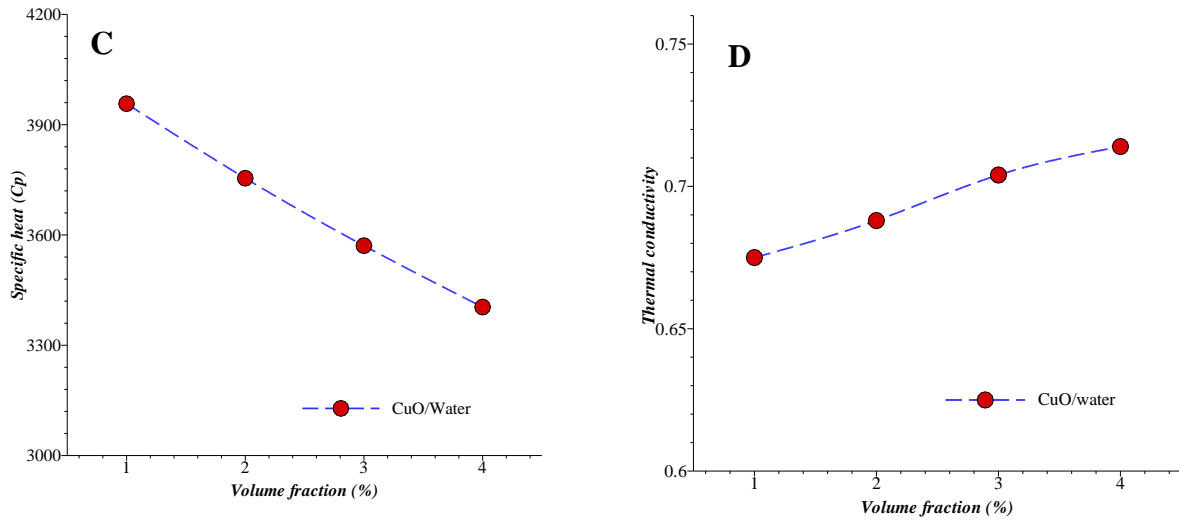


Fig. 7. CuO/water thermophysical properties at a different volume fraction

3. Experimental Data Reduction and Measurement Uncertainty Analysis

The following equations have been used in the experiment [37]:

The friction factor (f):

$$\Delta p = \Delta p_{in,out} - p_d \quad (3)$$

$$p_d = 1.18\rho u_{ave}^2 \quad (4)$$

$$u_{ave} = \frac{\dot{m}}{\rho A_c} \quad (5)$$

$$Re = \frac{u_{ave} \cdot D_h}{\nu} = \frac{\rho \cdot u_{ave} \cdot D_h}{\mu} \quad (6)$$

$$f = \Delta p \cdot \frac{D_h}{L} \cdot \frac{2}{\rho u_{ave}^2} \quad (7)$$

Power supply:

$$A_c = t \times W \quad (8)$$

$$R = \rho \times L / A_c \quad (9)$$

$$q = I^2 \times R \quad (10)$$

Nusselt Number (Nu):

$$A_s = L \times W \quad (11)$$

$$\Delta T = T_s - T_b \quad (12)$$

$$h = \frac{q}{A_s \times \Delta T} \quad (13)$$

$$Nu = \frac{h \times D_h}{k} \quad (14)$$

where

- Δp : The pressure drops
- u_{ave} : The average velocity
- D_h : Hydraulic diameter
- A_c : Cross section area
- L : Test section length
- W : The test section width
- h : Convective heat transfer coefficient (W/m².K)
- T_s : Surface temperature (K)
- T_b : Bulk temperature (K)
- ρ : Density of the working fluid (kg/m³)
- q : Heat transfer rate (W)
- R : Electrical resistance (Ω)

The precision of the results depends on the accuracy of each equipment used in the experimental setup. In the present study, the method by Kline and McClintock [38] has been employed to obtain uncertainty. The uncertainties of Nusselt number (Nu), friction factor, and Reynolds number (Re) which were observed from the experiment have been calculated [39,40].

Thus, the variable of the error value (R) can be determined as follows

$$R = f(x_1, x_2, \dots, x_n)$$

In the current research, the error values are recognisable for the values of the independent variables, which are (U_1, U_2, \dots, U_n). Consequently, the value of R can be estimated from the subsequent equations

$$U_R = \pm \left[\sum_{i=1}^n \left(\frac{\partial R}{\partial x_i} U_{x_i} \right)^2 \right]^{1/2} \quad (15)$$

where the uncertainty value is U_{x_i} for parameter x_i .

In the above equations, the quantity values and the measured parameter errors could be negative and positive. Hence the absolute value is deemed to determine the maximum amount of the uncertainty in the outcome of U_R . The uncertainty analysis for the Reynolds number (Re), Nusselt number (Nu), and friction factor (f) are ± 3.4 , ± 5.9 , and ± 7.8 , respectively. Besides, the accuracy of each instrument that been used in the present study has been tabulated in Table 1.

Table 1

Instruments and their accuracy

| Instruments | Accuracy |
|--------------------------------------|----------|
| K-type thermocouples | ± 0.3 |
| Pressure gauge | ± 0.05% |
| KD2 thermal analyzer | ±5% |
| Brookfield DV-II+ Viscometer | ± 0.03 |
| Different scanning calorimeter (DSC) | ±2% |
| Dwyer flow meter | ± 0.02 |
| Balance HR-250 AZ | ± 0.1 |
| BK 2831E 4 1/2 digital multimeter | ± 0.03% |
| Regulated power supply | ± 0.001 |

4. Results and Discussion

4.1 Flow Characteristics

The friction factor was experimentally calculated for the turbulent flow. The disparity between the experimental and numerical findings of the friction factor and its behaviour over the microscale backward-facing step (MBFS) are assessed. In the current experimental study, CuO nanoparticles are considered. To investigate the volume fraction (φ) effect on the flow of the fluid and the heat transfer, different values of CuO nanoparticles were chosen, which include 0, 0.01, 0.02, 0.03, and 0.04. The volume fraction (φ) impact on the friction factor is demonstrated in Figure 8.

Generally, Figure 8 shows that the rise in the Reynolds number (Re) leads to a decrease in the friction factor for all the concentrations utilised in this study. The outcomes demonstrated that increasing the nanoparticle volume fraction (φ) causes a remarkable increment in the friction factor. However, the findings of the numerical study illustrate that there is a minor variation in the friction factor of 0.01, 0.02, 0.03, and 0.04 volume fractions (φ) and pure water. Due to the increasing volume fraction (φ), the pressure drop is increased, which leads to an increase in the friction factor. Increasing the volume fraction (φ) leads to an increment in the viscosity of the nanofluid, which is related to the pressure drop.

The current study demonstrated that pure water has a smaller value of friction factor compared to the nanofluid of CuO/water. The increment of the friction factor is as a result of the high-density CuO nanoparticles compared to the small increase of the pure water pressure drop [42,43]. However, the numerical result showed that there is a slight change in the friction factor of CuO/water and pure water.

The effects of the volume fraction (φ) over the friction factor have been studied experimentally and numerically as shown in Figure 8. There exists a divergence between the experimental and numerical findings at the Reynolds number (Re) of 5,000. However, the current study detected that the deviation decreases at higher Re value.

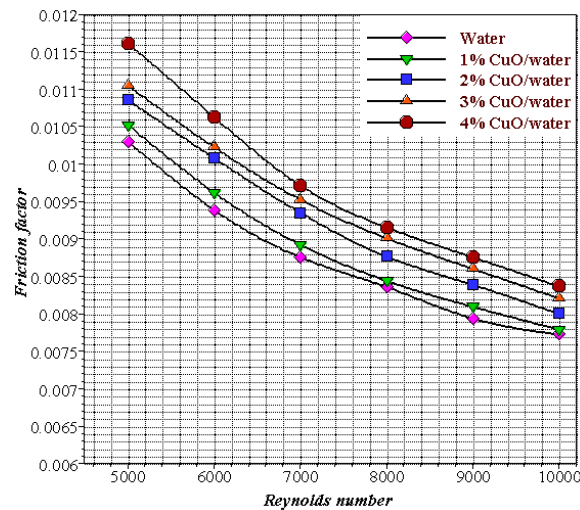


Fig. 8. Results of friction factor with different volume fractions (φ)

4.2 Heat Transfer Characteristics

The outcomes revealed a significant boost in the Nusselt number (Nu) utilising nanofluid. The maximum Nusselt number values begin downstream of the step where the recirculation and reattachment phenomenon happen and decreases all the way to the exit of the duct. In Figure 9, the impacts of utilising various volume fractions (φ) of CuO nanoparticles over the Nusselt number allocation alongside the x-coordinate is demonstrated.

The outcomes of the current study show that an improvement of 13.04% in the Nusselt number (Nu) was achieved when using 0.04 of CuO nanoparticles in comparison with only pure water. However, the percentage enhancement in the Nu is 4% by using 0.01 of CuO nanoparticles. Consequently, the experimental findings detected that the increment of the Nu is due to the increase in the volume fraction (φ) of CuO nanoparticles. These experimental findings show a rational agreement with the numerical outcomes, as demonstrated in Figure 9.

Different values of Reynolds number (Re) have been used to examine the impact on the Nusselt number (Nu). In the current study, pure water with 0.04 of CuO nanoparticle volume fraction (φ) is considered. In this study, three values of Re , 5,000, 7,000, and 10,000, are taken into consideration. The experimental outcomes revealed that by increasing the Re , an increment in the enhancement of the Nu occurred, as shown in Figure 10.

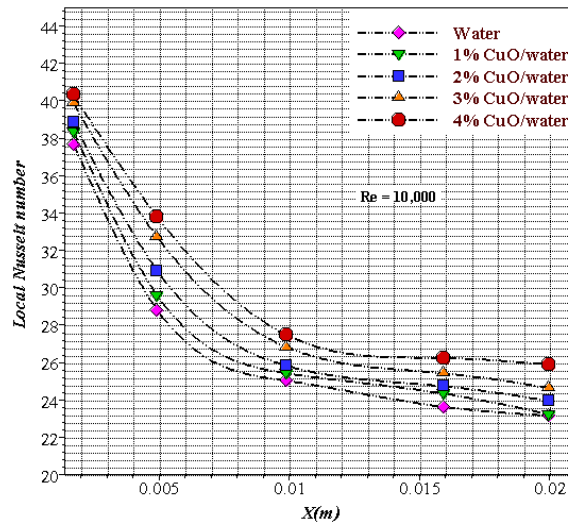


Fig. 9. Experimental results of volume fraction (φ) impacts on Nusselt number, (Nu)

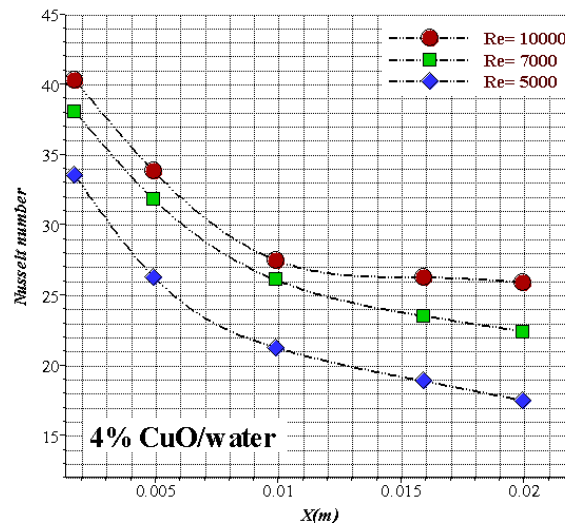


Fig. 10. Experimental results of Reynolds number (Re) impacts on Nusselt number (Nu)

This increment could be due to the following causes: (i) the low heat transfer rate in the microchannels and its amount are mostly critical and (ii) the influence by the low value of the bulk temperature. Therefore, as the Reynolds number (Re) increases, the diversity between the bulk temperature of the fluid and the temperature of the surface reduces. This demands high precision measuring devices. Moreover, the performance evaluation criteria (PEC) have been obtained to nominate the significant volume fraction that improved the heat transfer rate in comparison to the increasing percentage of the friction factor (f) [26]. Figure 11 shows the PEC of the CuO/ water nanofluid at different volume fraction. The equation of PEC as follow:

$$PEC = \left(\frac{Nu_{CuO-water}}{Nu_{Water}} \right) / \left(\frac{f_{CuO-water}}{f_{Water}} \right)^{\frac{1}{3}} \quad (16)$$

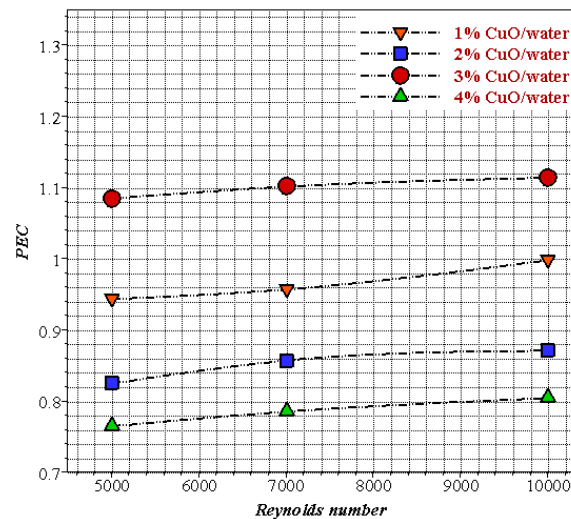


Fig. 11. Performance evaluation criteria (PEC) of using different CuO/water volume fractions

5. Conclusion

The results of the numerical and experimental study for the turbulent nanofluid over a flat horizontal duct with a microscale backward-facing step (MBFS) were demonstrated. CuO nanoparticles with water were considered as the base fluid. The evaluations were obtained based on the Reynolds numbers (Re) and volume fractions (φ) of the turbulent nanofluid flow. The findings can be concluded as follows

- i. The heat transfer rate enhances with an increase in any of the parameters of volume fraction (φ) and Reynolds number (Re). Also, the friction factor has a significant consequence on the rate of heat transfer and characteristics of the flow at a constant Re .
- ii. In all cases of the volume fractions (φ), the outcomes revealed that the friction factor is reduced by boosting the Reynolds number (Re). However, the rise in the φ caused an increment in the friction factor.
- iii. The effectiveness as shown by the Nusselt number (Nu) increases by increasing the volume fraction (φ) of the nanoparticles. In contrast with pure water, the current study showed an improvement of 13.04% in the Nu by applying a nanofluid of CuO/water with a 0.04 φ of CuO nanoparticles.
- iv. SEM, particle size distribution and XRD have been applied to ensure the purity of the CuO nanoparticles used in the current study.

Acknowledgement

The research was funded under the MySIP grant scheme no. 5540547 from Ministry of Higher Education Malaysia.

References

- [1] Togun, Hussein. "Effect of laminar separation flow and nanofluids on heat transfer augmentation with passive techniques: A review." *International Communications in Heat and Mass Transfer* 77 (2016): 9-14. <https://doi.org/10.1016/j.icheatmasstransfer.2016.07.009>
- [2] Hamid, Mohd Faisal Abdul. "Review of improvements on heat transfer using nanofluids via corrugated facing step." *International Journal of Engineering & Technology* 7, no. 4.13 (2018): 160-169. <https://doi.org/10.14419/ijet.v7i4.13.21350>
- [3] Sharaf, Hussein Kadhim, Sadeq Salman, Mohammad Hassan Dindarloo, Valery I. Kondrashchenko, Alla

- Andronikovna Davidyants, and Sergey V. Kuznetsov. "The effects of the viscosity and density on the natural frequency of the cylindrical nanoshells conveying viscous fluid." *The European Physical Journal Plus* 136, no. 1 (2021): 1-19. <https://doi.org/10.1140/epjp/s13360-020-01026-y>
- [4] Talib, Abd Rahim Abu, and Ali Kareem Hilo. "Fluid flow and heat transfer over corrugated backward facing step channel." *Case Studies in Thermal Engineering* 24 (2021): 100862. <https://doi.org/10.1016/j.csite.2021.100862>
- [5] Hilo, Ali Kareem, Antonio Acosta Iborra, Mohammed Thariq Hameed Sultan, and Mohd Faisal Abdul Hamid. "Effect of corrugated wall combined with backward-facing step channel on fluid flow and heat transfer." *Energy* 190 (2020): 116294. <https://doi.org/10.1016/j.energy.2019.116294>
- [6] Hilo, Ali, Sadeq Rashid Nfawa, Mohamed Thariq Hameed Sultan, Mohd Faisal Abdul Hamid, and M. I. Nadiir Bheekhun. "Heat transfer and thermal conductivity enhancement using graphene nanofluid: a review." *Journal of Advanced Research in Fluid Mechanics and Thermal Sciences* 55, no. 1 (2019): 74-87.
- [7] Ashham, M., H. K. Sharaf, K. Salman, and S. Salman. "Simulation of heat transfer in a heat exchanger tube with inclined vortex rings inserts." *International Journal of Applied Engineering* 12, no. 20 (2017): 9605-9613.
- [8] Abu-Mulaweh, H. I., Bassem F. Armaly, and T. S. Chen. "Laminar natural convection flow over a vertical forward-facing step." *Journal of Thermophysics and Heat Transfer* 10, no. 3 (1996): 517-523. <https://doi.org/10.2514/3.819>
- [9] Abu-Mulaweh, H. I., Bassem F. Armaly, and T. S. Chen. "Measurements of laminar mixed convection in boundary-layer flow over horizontal and inclined backward-facing steps." *International Journal of Heat and Mass Transfer* 36, no. 7 (1993): 1883-1895. [https://doi.org/10.1016/S0017-9310\(05\)80176-0](https://doi.org/10.1016/S0017-9310(05)80176-0)
- [10] Abu-Mulaweh, H. I., T. S. Chen, and Bassem F. Armaly. "Turbulent mixed convection flow over a backward-facing step--the effect of the step heights." *International Journal of Heat and Fluid Flow* 23, no. 6 (2002): 758-765. [https://doi.org/10.1016/S0142-727X\(02\)00191-1](https://doi.org/10.1016/S0142-727X(02)00191-1)
- [11] Abu-Mulaweh, H. I., Bassem F. Armaly, and T. S. Chen. "Measurements in buoyancy-assisting laminar boundary layer flow over a vertical backward-facing step-uniform wall heat flux case." *Experimental Thermal and Fluid Science* 7, no. 1 (1993): 39-48. [https://doi.org/10.1016/0894-1777\(93\)90079-X](https://doi.org/10.1016/0894-1777(93)90079-X)
- [12] Nie, J. H., and Bassem F. Armaly. "Three-dimensional convective flow adjacent to backward-facing step-effects of step height." *International Journal of Heat and Mass Transfer* 45, no. 12 (2002): 2431-2438. [https://doi.org/10.1016/S0017-9310\(01\)00345-3](https://doi.org/10.1016/S0017-9310(01)00345-3)
- [13] Armaly, B. F., A. Li, and J. H. Nie. "Three-dimensional forced convection flow adjacent to backward-facing step." *Journal of Thermophysics and Heat Transfer* 16, no. 2 (2002): 222-227. <https://doi.org/10.2514/2.6688>
- [14] Chen, Y. T., J. H. Nie, B. F. Armaly, and Hsuan-Tsung Hsieh. "Turbulent separated convection flow adjacent to backward-facing step-effects of step height." *International Journal of Heat and Mass Transfer* 49, no. 19-20 (2006): 3670-3680. <https://doi.org/10.1016/j.ijheatmasstransfer.2006.02.024>
- [15] Kherbeet, A. Sh, H. A. Mohammed, K. M. Munisamy, and B. H. Salman. "The effect of step height of microscale backward-facing step on mixed convection nanofluid flow and heat transfer characteristics." *International Journal of Heat and Mass Transfer* 68 (2014): 554-566. <https://doi.org/10.1016/j.ijheatmasstransfer.2013.09.050>
- [16] Mohammed, Hussein A., A. A. Al-Aswadi, Mohd Zamri Yusoff, and Rahman Saidur. "Buoyancy-assisted mixed convective flow over backward-facing step in a vertical duct using nanofluids." *Thermophysics and Aeromechanics* 19, no. 1 (2012): 33-52. <https://doi.org/10.1134/S0869864312010040>
- [17] Ajeel, Raheem K., K. Sopian, Rozli Zulkifli, Saba N. Fayyadh, and Ali Kareem Hilo. "Assessment and analysis of binary hybrid nanofluid impact on new configurations for curved-corrugated channel." *Advanced Powder Technology* 32, no. 10 (2021): 3869-3884. <https://doi.org/10.1016/j.apt.2021.08.041>
- [18] Lv, Jizu, Chengzhi Hu, Minli Bai, Liangyu Li, Lin Shi, and Dongdong Gao. "Visualization of SiO₂-water nanofluid flow characteristics in backward-facing step using PIV." *Experimental Thermal and Fluid Science* 101 (2019): 151-159. <https://doi.org/10.1016/j.expthermflusci.2018.10.013>
- [19] Hilo, Ali Kareem, Antonio Acosta Iborra, Mohammed Thariq Hameed Sultan, and Mohd Faisal Abdul Hamid. "Experimental study of nanofluids flow and heat transfer over a backward-facing step channel." *Powder Technology* 372 (2020): 497-505. <https://doi.org/10.1016/j.powtec.2020.06.013>
- [20] Nath, Ratnadeep, and Murugesan Krishnan. "Numerical study of double diffusive mixed convection in a backward facing step channel filled with Cu-water nanofluid." *International Journal of Mechanical Sciences* 153 (2019): 48-63. <https://doi.org/10.1016/j.ijmecsci.2019.01.035>
- [21] Kherbeet, A. Sh, H. A. Mohammed, B. H. Salman, Hamdi E. Ahmed, and Omer A. Alawi. "Experimental and numerical study of nanofluid flow and heat transfer over microscale backward-facing step." *International Journal of Heat and Mass Transfer* 79 (2014): 858-867. <https://doi.org/10.1016/j.ijheatmasstransfer.2014.08.074>
- [22] Kherbeet, A. Sh, H. A. Mohammed, B. H. Salman, Hamdi E. Ahmed, Omer A. Alawi, and M. M. Rashidi. "Experimental study of nanofluid flow and heat transfer over microscale backward-and forward-facing steps." *Experimental Thermal and Fluid Science* 65 (2015): 13-21. <https://doi.org/10.1016/j.expthermflusci.2015.02.023>
- [23] Kherbeet, A. Sh, H. A. Mohammed, and B. H. Salman. "The effect of nanofluids flow on mixed convection heat

- transfer over microscale backward-facing step." *International Journal of Heat and Mass Transfer* 55, no. 21-22 (2012): 5870-5881. <https://doi.org/10.1016/j.ijheatmasstransfer.2012.05.084>
- [24] Al-Aswadi, A. A., H. A. Mohammed, N. H. Shuaib, and Antonio Campo. "Laminar forced convection flow over a backward facing step using nanofluids." *International Communications in Heat and Mass Transfer* 37, no. 8 (2010): 950-957. <https://doi.org/10.1016/j.icheatmasstransfer.2010.06.007>
- [25] Selimefendigil, Fatih, and Hakan F. Öztop. "Influence of inclination angle of magnetic field on mixed convection of nanofluid flow over a backward facing step and entropy generation." *Advanced Powder Technology* 26, no. 6 (2015): 1663-1675. <https://doi.org/10.1016/j.appt.2015.10.002>
- [26] Abu Talib, Abd Rahim, and Sadeq Salman. "Heat transfer and fluid flow analysis over the microscale backward-facing step using β Ga₂O₃ nanoparticles." *Experimental Heat Transfer* (2022): 1-18. <https://doi.org/10.1080/08916152.2022.2039328>
- [27] Abu-Nada, Eiyad. "Application of nanofluids for heat transfer enhancement of separated flows encountered in a backward facing step." *International Journal of Heat and Fluid Flow* 29, no. 1 (2008): 242-249. <https://doi.org/10.1016/j.ijheatfluidflow.2007.07.001>
- [28] Kherbeet, A. Sh, H. A. Mohammed, K. M. Munisamy, and B. H. Salman. "Effect of base fluid on mixed convection nanofluid flow over microscale backward-facing step." *Journal of Computational and Theoretical Nanoscience* 12, no. 10 (2015): 3076-3089. <https://doi.org/10.1166/jctn.2015.4083>
- [29] Mehrez, Zouhaier, Mourad Bouterra, Afif El Cafsi, Ali Belghith, and Patrick Le Quere. "The influence of the periodic disturbance on the local heat transfer in separated and reattached flow." *Heat and Mass Transfer* 46, no. 1 (2009): 107-112. <https://doi.org/10.1007/s00231-009-0548-z>
- [30] Labbé, Odile, Pierre Sagaut, and Emmanuel Montreuil. "Large-eddy simulation of heat transfer over a backward-facing step." *Numerical Heat Transfer: Part A: Applications* 42, no. 1-2 (2002): 73-90. <https://doi.org/10.1080/10407780290059431>
- [31] Abu-Mulaweh, H. I., T. S. Chen, and Bassem F. Armaly. "Turbulent mixed convection flow over a backward-facing step--the effect of the step heights." *International Journal of Heat and Fluid Flow* 23, no. 6 (2002): 758-765. [https://doi.org/10.1016/S0142-727X\(02\)00191-1](https://doi.org/10.1016/S0142-727X(02)00191-1)
- [32] Nie, J. H., and B. F. Armaly. "Reverse flow regions in three-dimensional backward-facing step flow." *International Journal of Heat and Mass Transfer* 47, no. 22 (2004): 4713-4720. <https://doi.org/10.1016/j.ijheatmasstransfer.2004.05.027>
- [33] Gavasane, Abhimanyu, Amit Agrawal, and Upendra Bhandarkar. "Study of rarefied gas flows in backward facing micro-step using Direct Simulation Monte Carlo." *Vacuum* 155 (2018): 249-259. <https://doi.org/10.1016/j.vacuum.2018.06.014>
- [34] Hsieh, Tse-Yang, Zuu-Chang Hong, and Ying-Che Pan. "Flow characteristics of three-dimensional microscale backward-facing step flows." *Numerical Heat Transfer, Part A: Applications* 57, no. 5 (2010): 331-345. <https://doi.org/10.1080/10407780903582992>
- [35] Salman, Sadeq, Ali Hilo, Sadeq Rashid Nfawa, Mohamed Thariq Hameed Sultan, and Syamimi Saadon. "Numerical study on the turbulent mixed convective heat transfer over 2D microscale backward-facing step." *CFD Letters* 11, no. 10 (2019): 31-45.
- [36] Salman, S., A. R. Abu Talib, S. Saadon, and M. T. Hameed Sultan. "Hybrid nanofluid flow and heat transfer over backward and forward steps: A review." *Powder Technology* 363 (2020): 448-472. <https://doi.org/10.1016/j.powtec.2019.12.038>
- [37] Siddiqui, Vasi Uddin, Afzal Ansari, Ruchi Chauhan, and Weqar Ahmad Siddiqi. "Green synthesis of copper oxide (CuO) nanoparticles by Punica granatum peel extract." *Materials Today: Proceedings* 36 (2021): 751-755. <https://doi.org/10.1016/j.matpr.2020.05.504>
- [38] Kline, S. A., and F. A. McClintock. "Describing Uncertainties in Single-Sample Experiments." *Mechanical Engineering* 75 (1953): 3-8.
- [39] Holman, Jack Philip. *Experimental methods for engineers*. 7th ed. McGraw-Hill, 2001.
- [40] Mohammed, Hussein A., and Yasin K. Salman. "Experimental investigation of mixed convection heat transfer for thermally developing flow in a horizontal circular cylinder." *Applied Thermal Engineering* 27, no. 8-9 (2007): 1522-1533. <https://doi.org/10.1016/j.applthermaleng.2006.09.023>
- [41] Ahmed, Hamdi E., Mirghani Ishak Ahmed, and Mohd Zamri Yusoff. "Heat transfer enhancement in a triangular duct using compound nanofluids and turbulators." *Applied Thermal Engineering* 91 (2015): 191-201. <https://doi.org/10.1016/j.applthermaleng.2015.07.061>
- [42] Kherbeet, A. Sh, H. A. Mohammed, B. H. Salman, Hamdi E. Ahmed, and Omer A. Alawi. "Experimental and numerical study of nanofluid flow and heat transfer over microscale backward-facing step." *International Journal of Heat and Mass Transfer* 79 (2014): 858-867. <https://doi.org/10.1016/j.ijheatmasstransfer.2014.08.074>
- [43] Moghari, R. Mokhtari, A. Akbarinia, M. Shariat, F. Talebi, and R. Laur. "Two phase mixed convection Al₂O₃-water

- nanofluid flow in an annulus." *International Journal of Multiphase Flow* 37, no. 6 (2011): 585-595. <https://doi.org/10.1016/j.ijmultiphaseflow.2011.03.008>
- [44] Shariat, Mohammad, Alireza Akbarinia, Alireza Hossein Nezhad, Amin Behzadmehr, and Rainer Laur. "Numerical study of two phase laminar mixed convection nanofluid in elliptic ducts." *Applied Thermal Engineering* 31, no. 14-15 (2011): 2348-2359. <https://doi.org/10.1016/j.applthermaleng.2011.03.035>